2012 IEEE International Conference on Robotics and Automation
RiverCentre, Saint Paul, Minnesota, USA
May 14-18, 2012

High-speed Flight in an Ergodic Forest

Sertac Karaman Emilio Frazzoli

Abstract— **Inspired by birds flying through cluttered environments such as dense forests, this paper studies the theoretical foundations of high-speed motion through a randomly-generated obstacle field. Assuming that the locations and the sizes of the trees are determined by an ergodic point process, and under mild technical conditions on the dynamics of the bird, it is shown that the existence of an infinite collision-free trajectory through the forest exhibits a phase transition. In other words, if the bird flies faster than a certain critical speed, there is no infinite collision-free trajectory, with probability one, i.e., the bird will eventually collide with some tree, almost surely, regardless of the planning algorithm governing its motion. On the other hand, if the bird flies slower than this critical speed, then there exists at least one infinite collision-free trajectory, almost surely. Lower and upper bounds on the critical speed are derived for the special case of a Poisson forest considering a simple model for the bird's dynamics. Moreover, results from an extensive Monte-Carlo simulation study are presented. This paper also establishes novel connections between robot motion planning and statistical physics through ergodic theory and the theory of percolation, which may be of independent interest.**

I. Introduction

Flying or land-based, high-performance robots that can quickly navigate through cluttered environments, such as urban canyons and dense forests, have long been an objective of robotics research [1]–[6], although very little could have been established in realizing them so far. Yet, nature is home to several species of birds that are capable of flying at high speeds in densely cluttered environments, such as forests, as a part of their daily rituals [7].

Biologist have studied birds both theoretically and experimentally for decades, establishing a good understanding of their behavior during various activities such as foraging, migration, and food transport [8]. In particular, the optimal speed at which a bird should fly during steady flight, e.g., to minimize the energy dissipated, has been studied extensively [8]–[13]. However, birds' flight in cluttered environments has received relatively little attention, although many birds inhabit dense forests. Recently, Hedrick and Biewener [12], [13] argued that the historical focus on steady flight may be due to its theoretical and experimental tractability, rather than its importance.

Inspired by various applications in robotics and biology, in this paper, we study the theoretical foundations of a novel motion planning problem: high-speed navigation in a randomly-generated obstacle field with known statistics. We motivate this problem by a bird flying in a planar forest environment. We model the forest using a marked point process that generates the locations and the sizes of the trees in the forest, and we represent the dynamics of the bird by an ordinary differential equation parametrized by a speed variable. We then ask the following question: *what is the maximum speed at which flight can be maintained indefinitely with probabilistic guarantees, e.g., almost surely?*

In the case when the forest generating process is ergodic, the answer turns out to be tied to a novel phase transition result, showing the existence of a critical speed such that: on one hand, for any speed above critical there is no infinite collision-free trajectory, with probability one; on the other hand, for any speed lower than the critical speed, there exists at least one infinite collision-free trajectory, with probability one. In this context, a trajectory is said to be infinite, if it can not be contained in any bounded subset of the plane.

Let us note that spatial point processes are widely used in the context of forestry [14]. In fact, Stoyan [15] noted that no other application area "uses point process methods so intensively, and stimulated the theory so much, as has forestry." In particular, the Poisson process model has been used extensively to represent the distribution of trees in a forest stand [15]. Indeed, Tomppo found that around 30% of the inventory plots in Finland could be considered as a realization of a Poisson point process [16]. Apart from Poisson processes, forestry literature has extensively used, e.g., cluster processes, Cox processes, and Gibbs processes, most of which are ergodic or have ergodic variants.

The contributions of this paper can be listed as follows. First, it is shown that, under mild technical assumptions on the dynamics governing the bird, the existence of infinite collision-free trajectories traversing an ergodic forest exhibits a phase transition. More precisely, in that case, there exists a critical speed, ν_{crit}, such that: (i) for any speed $\nu < \nu_{\mathrm{crit}}$, flight with speed ν can be maintained indefinitely while increasingly getting away from some initial condition, with probability one; (ii) for any speed $\nu > \nu_{\mathrm{crit}}$, the bird will eventually collide with a tree, almost surely, despite complete knowledge of the tree locations, regardless of the algorithm used to plan the bird's motion. Second, the special case in which the bird is governed by a simple dynamic model and the forest is generated by a homogeneous spatial Poisson point process with intensity ρ, and is such that all trees have a fixed radius r is considered. Non-trivial lower and upper bounds for the critical speed is derived for any pair of ρ and r. Third, the results of extensive Monte-Carlo simulations are presented for the same special case. The simulation study confirms the aforementioned striking phase transition.

These results lay down the theoretical foundations of a novel class of motion planning problems involving high-speed motion in a randomly-generated obstacle field, where

Laboratory for Information and Decision Systems, Massachusetts Institute of Technology, Cambridge, MA. {sertac,frazzoli}@mit.edu

the statistics of the obstacle generation process are known, but, for instance, the precise location and the shape of the obstacles are not known *a priori*. Our analysis implies strong negative results showing that under certain conditions collision-free motion above a critical speed is impossible to maintain indefinitely, with probability one.

Finally, the analysis in this paper hinges on novel connections between robot motion planning and statistical physics, in particular the ergodic theory [17] and the theory of percolation [18], [19]. In fact, our work constitutes one of the few examples where such theory is employed with the purpose of designing engineering systems such as high-speed robotic vehicles, rather than studying physical phenomena.

This paper is organized as follows. In Section II, the forest generating process and the dynamics governing the bird are described. The main result on phase transitions in ergodic forests is stated and proven in Section III. In Section IV, the Poisson forest model is introduced and an upper bound on the critical speed is derived using continuum percolation theory. Computational experiments are presented in Section V. The paper is concluded with remarks in Section VI.

II. The Forest, The Bird, and The Problem

In this section, fairly general forest and bird models are introduced, and a formal problem definition is provided. An important special case of the problem is also discussed.

A. The Forest-generating Process

Consider a planar forest environment modeled by a marked point process, where the points represent the locations and the marks represent the sizes of the trees. We postpone a formal treatment of such processes till Section III. To provide a problem definition free of the measure-theoretic formalism, in this section, we define the *forest-generating process* as a random set $\{(y_i, r_i) : i \in \mathbb{N}\}$, where $y_i \in \mathbb{R}^2$ denotes the location and $r_i \in \mathbb{R}_{>0}$ denotes the radius of tree i.

Let Ω denote the underlying sample space. A realization of the forest-generating process is denoted by $F(\omega)$, where $\omega \in \Omega$. Given a realization $F(\omega) = \{(y_i, r_i) : i \in \mathbb{N}\}$ of the forest, define the *region occupied by the trees* as $\mathcal{X}_{\text{trees}}^{F(\omega)} := \bigcup_{i\in\mathbb{N}} B_{r_i}(y_i)$, where $B_r(y) \subset \mathbb{R}^2$ is the disk-shaped region of radius r centered at y. Define the *free region* as $\mathcal{X}_{\text{free}}^{F(\omega)} := \mathbb{R}^2 \setminus \mathcal{X}_{\text{trees}}^{F(\omega)}$. Note that $\mathcal{X}_{\text{trees}}^{F}$ and $\mathcal{X}_{\text{free}}^{F}$ are random sets.

B. The Model of the Bird

Let $\mathcal{X} \subseteq \mathbb{R}^n$ and $\mathcal{U} \subseteq \mathbb{R}^m$ be measurable sets, where $n, m \in \mathbb{N}$. Consider a collection of dynamical systems, parametrized by a speed variable $\nu \in \mathbb{R}_{>0}$, given by

$$\begin{aligned} \dot{x}(t) = f_\nu(x(t), u(t)), \quad x(0) = x_0, \\ y(t) = h_\nu(x(t)), \end{aligned} \tag{1}$$

where $f_\nu : \mathcal{X} \times \mathcal{U} \to \mathbb{R}^n$ and $h_\nu : \mathcal{X} \to \mathbb{R}^2$ are Lipschitz continuous in both variables for all ν, and $x(t) \in \mathcal{X}$ and $u(t) \in \mathcal{U}$ for all t. A function $y : \mathbb{R}_{\geq 0} \to \mathbb{R}^2$ is said to be a trajectory of the system described by Equation (1) at speed ν if there exist measurable functions $u : \mathbb{R}_{\geq 0} \to \mathcal{U}$ and $x : \mathbb{R}_{\geq 0} \to \mathcal{X}$ such that u, x, and y satisfy Equation (1). The family of all trajectories at speed ν is denoted by Γ_ν.

C. Problem Definition

A trajectory $y \in \Gamma_\nu$, for some ν, is said to be *infinite* if $\liminf_{t\to\infty} \|y(t)\| = \infty$, where $\|\cdot\|$ denotes the usual Euclidean norm in $\mathbb{R}^2$. The trajectory is said to be *collision free* in a particular realization $F(\omega)$ of the forest, if $y(t) \in \mathcal{X}_{\text{free}}^{F(\omega)}$ for all $t \in \mathbb{R}_{\geq 0}$. This paper is concerned with the existence of infinite collision-free trajectories.

D. A Single-integrator Bird Flying in a Poisson Forest

Recall that the dynamics of the bird was described by Equation (1). Consider the following special case:

$$\begin{aligned} \dot{x}(t) = f_\nu(x(t), u(t)) = \begin{pmatrix} \nu \\ u(t) \end{pmatrix}, \\ y(t) = h_\nu(x(t)) = x(t), \end{aligned} \tag{2}$$

where $x(t), y(t) \in \mathbb{R}^2$ and $u(t) \in [-1, 1]$ for all $t \geq 0$. According to this model, the bird is flying at a constant speed, denoted by ν, in the longitudinal direction, while it can maneuver with bounded speed in the lateral direction.

The equation describing the dynamics prescribed by Equation (2) is parametrized by ν, which denotes the "speed" parameter, although in this case ν is not precisely the speed of the bird, but rather its speed in the longitudinal direction.

The set of states reachable at or before time t for this system is a cone-shaped region shown in Figure 1. An important parameter in the analysis of this model turns out to be the aperture of this cone defined as $\alpha := 2\tan^{-1}(1/\nu)$. Roughly speaking, α corresponds to the "maneuverability" of the bird; increasing values of α correspond to larger reachable sets, thus more maneuvering ability for the bird.

Recall that $P(A)$ denotes the number of points of the point process P that fall into the Borel set $A \subset \mathbb{R}^2$. Then, P is said to be a *(homogeneous) Poisson process* with intensity λ, if (i) for all pairwise disjoint Borel sets $A_1, A_2, \ldots, A_n$, the random variables $P(A_1), P(A_2), \ldots, P(A_n)$ are mutually independent, and (ii) for every bounded Borel set A, the random variable $P(A)$ is a Poisson random variable with mean $\lambda\,\mu(A)$, where $\mu(\cdot)$ is the usual Lebesgue measure. A Poisson point process with intensity λ is denoted by Π_λ.

In what follows, we focus on the special case when the bird described by Equation (2) is flying in a forest, where the locations of the trees are generated by the process Π_ρ and their radii are all equal to $r > 0$. Throughout the paper, this forest-generating process is called the *Poisson forest-generating process* with tree density ρ and the tree radius r, and the bird model given by Equation (2) is called the *single-integrator bird* flying at speed ν.

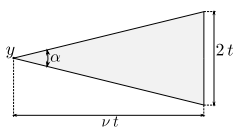

Fig. 1. The set of states reachable from $y \in \mathbb{R}^2$ within time t.

III. Phase Transitions in Ergodic Forests

In this section, ergodic forest-generating processes are defined and the phase transition result is proven.

A. Ergodic Forest-generating Processes

Let $\mathcal{B}(\mathbb{R})$ denote the set of all Borel subsets of $\mathbb{R}$. The set $\mathcal{B}(\mathbb{R}^2)$ is defined similarly. A *Borel measure* on $\mathbb{R}^2$ is a function, usually denoted by ξ, that maps $\mathcal{B}(\mathbb{R}^2)$ to $\mathbb{R}$ such that it is nonnegative, i.e., $\xi(A) \geq 0$ for all $A \in \mathcal{B}(\mathbb{R}^2)$, and σ-additive, i.e., $\xi(\cup_{i\in\mathbb{N}} A_i) = \sum_{i\in\mathbb{N}} \xi(A_i)$ for any sequence $\{A_i\}_{i\in\mathbb{N}}$ of disjoint Borel sets. A Borel measure ξ on $\mathbb{R}^2$ is said to be *boundedly finite* if $\xi(A) < \infty$ for all bounded $A \in \mathcal{B}(\mathbb{R}^2)$. A *counting measure* n is an integer-valued boundedly finite Borel measure, i.e., $n(A) \in \mathbb{Z}$ for all $A \in \mathcal{B}(\mathbb{R}^2)$. The space of all counting measures on $\mathbb{R}^2$ is denoted by $\mathcal{N}$. The set of all Borel subsets of $\mathcal{N}$ is denoted by $\mathcal{B}(\mathcal{N})$.

Let $(\Omega, \mathcal{F}, \mathbb{P})$ be a probability space. A *point process* P is a measurable mapping from Ω to $\mathcal{N}$, i.e., for all $N \in \mathcal{B}(\mathcal{N})$, $P^{-1}(N) := \{\omega \in \Omega : P(\omega) \in N\} \in \mathcal{F}$. Defined in this way, P assigns a counting measure $n = P(\omega) \in \mathcal{N}$ to any sample path $\omega \in \Omega$, such that $n(A)$ is the number of points that fall into $A \in \mathcal{B}(\mathbb{R}^2)$. Thus, P randomly generates a counting measure that counts the number of points in any given Borel subset of the plane. Given any Borel set $A \in \mathcal{B}(\mathbb{R}^2)$, the number of points that fall into A in the point process P, denoted by $P(A)$ with a slight abuse of notation, is an integer-valued random variable.

Let $\mathcal{K}$ be a mark space. Let $\mathcal{M}_\mathcal{K}$ denote the set of counting measures on the space $\mathbb{R}^2 \times \mathcal{K}$ of point-mark pairs. Then, a (spatial) *marked point process* Q is a measurable mapping from a probability space $(\Omega, \mathcal{F}, \mathbb{P})$ to $\mathcal{M}_\mathcal{K}$ such that the *ground measure*, defined by $Q_g(A) = Q(A\times K)$ for all $A \in \mathcal{B}(\mathbb{R}^2)$, is a boundedly finite counting measure for all $K \in \mathcal{B}(\mathcal{K})$. Defined in this way, a marked point process assigns a counting measure $m = Q(\omega) \in \mathcal{M}_\mathcal{K}$ such that $m(B)$ denotes the the number of points y with mark k such that $(y, k) \in B$, for all $B \in \mathcal{B}(\mathbb{R}^2 \times \mathcal{K})$. In particular, $m(A\times K)$ denotes the number of points in $A \in \mathcal{B}(\mathbb{R}^2)$ with marks in $K \in \mathcal{B}(\mathcal{K})$. Finally, a *forest-generating process*, usually denoted by F, is a marked point process defined on a mark space $\mathcal{K} = \mathbb{R}_{>0}$, where marks denote the radii of the trees.

For all $v, y \in \mathbb{R}^2$, all $k \in \mathcal{K}$, and all $B \in \mathcal{B}(\mathbb{R}^2 \times \mathcal{K})$, define the *translation operator* T_v as $T_v(y, k) := (y + v, k)$ and $T_v B := \{(y + v, k) : (y, k) \in B\}$. Intuitively, given a set B of marked points in the plane, the translation operator T_v applied to B translates the location of all points by a vector v while keeping their marks the same. The operator T_v induces a transformation S_v on $\mathcal{M}_\mathcal{K}$, defined as $(S_v m)(B) = m(T_v B)$ for all $v \in \mathbb{R}^2$, all $B \in \mathcal{B}(\mathbb{R}^2 \times \mathcal{K})$, and all $m \in \mathcal{M}_\mathcal{K}$. Clearly, the space $\mathcal{M}_\mathcal{K}$ of all counting measures on $\mathbb{R}^2 \times \mathcal{K}$ is closed under this transformation, i.e., $S_v m \in \mathcal{M}_\mathcal{K}$ for all $m \in \mathcal{M}_\mathcal{K}$. Thus, this transformation is naturally generalized to any marked point process by defining $(S_v Q)(\omega) = S_v(Q(\omega))$ for all $\omega \in \Omega$, which makes $S_v Q : \Omega \to \mathcal{M}_\mathcal{K}$ a measurable mapping for any $v \in \mathbb{R}^2$. Hence, the translated marked point process, $S_v Q$, is a marked point process on its own right.

Every marked point process Q induces a probability measure on the measure space $(\mathcal{M}_\mathcal{K}, \mathcal{B}(\mathcal{M}_\mathcal{K}))$, defined as $\mathcal{P}_Q(M) := \mathbb{P}(Q^{-1}(M))$ for all $M \in \mathcal{B}(\mathcal{M}_\mathcal{K})$. The probability measure $\mathcal{P}_Q$ is called the *distribution* of Q. A marked point process Q is said to be *stationary* if its distribution is invariant under the set $\{S_v : v \in \mathbb{R}^2\}$ of transformations, i.e., $\mathcal{P}_Q(M) = \mathcal{P}_{S_v Q}(M)$ for all $M \in \mathcal{B}(\mathcal{M}_\mathcal{K})$. In other words, Q is said to be stationary if the family $\{S_v Q : v \in \mathbb{R}^2\}$ of marked point processes have the same distribution. Finally, a stationary marked point process Q is said to be *ergodic* if

$$\lim_{a\to\infty} \frac{1}{a^2} \int_{[0,a]^2} \mathcal{P}_Q((S_v M_1) \cap M_2) dv = \mathcal{P}_Q(M_1)\, \mathcal{P}_Q(M_2),$$

for all $M_1, M_2 \in \mathcal{B}(\mathcal{M}_\mathcal{K})$. A forest-generating process is *ergodic*, if its corresponding marked point process is ergodic.

Ergodic point processes admit an important characterization through their invariant sigma-algebra being trivial. In this context, an event $M \in \mathcal{B}(\mathcal{M}_\mathcal{K})$ is said to be *invariant* under the transformation S_u, if $S_u^{-1} M = M$. It can be shown that the set $\mathcal{I}$ of all events in $\mathcal{B}(\mathcal{M}_\mathcal{K})$ that are invariant under the family $\{S_u : u \in \mathbb{R}^2\}$ of transformations is indeed a σ-algebra [20]. The set $\mathcal{I}$ is said to be *trivial* if $\mathcal{P}_Q(M) \in \{0, 1\}$ for all $M \in \mathcal{I}$. The following theorem is a central result in the theory of ergodic point processes.

Theorem 1 ([20]) *A marked point process Q is ergodic if and only if $\mathcal{I}$, the set of events invariant under transformations $\{S_v : v \in \mathbb{R}^2\}$, is trivial under the distribution of Q.*

The reader is referred to [21] for a detailed discussion of ergodic point processes.

B. The Monotonic Zero-One Law of the Ergodic Forest

Recall that Γ_ν denotes the set of all dynamically feasible trajectories of the bird when flying at speed ν. The dynamics of the bird is said to be *translation invariant*, if any dynamically-feasible trajectory is still dynamically feasible when translated as a whole. More precisely, the bird has translation-invariant dynamics, if for all $y \in \Gamma_\nu$ and all $y_0 \in \mathbb{R}^2$, the translated trajectory y', defined by $y'(t) := y(t)+y_0$ for all $t \in [0, T]$, satisfies $y' \in \Gamma_\nu$. Roughly speaking, this assumption implies that the dynamics of the bird does not depend on a particular location in the forest.

This section is concerned with the existence of an infinite collision-free trajectory for the bird, described by the event

$$E_F(\nu) := \big\{\text{there exists a trajectory } y \in \Gamma_\nu \text{ such that } \lim_{t\to\infty} \|y(t)\|_2 = \infty \text{ and } y(t) \in \mathcal{X}_{\text{free}}^F \text{ for all } t \in \mathbb{R}_{>0}\big\}.$$

The following intermediate result establishes a zero-one law assuming that the forest-generating process is ergodic.

Lemma 2 *Let F be a forest-generating process and suppose that the dynamics governing the bird is translation invariant. Then, $\mathbb{P}(E_F(\nu)) \in \{0, 1\}$ for all ν, whenever the forest-generating process is ergodic.*

The bird is said to have *non-decreasing path sets with decreasing speed*, if any dynamically-feasible trajectory can

be retraced, albeit with a reparametrization of time, at a lower speed. That is, for any $\nu, \nu' \in \mathbb{R}_{>0}$ with $\nu' < \nu$, and any $y \in \Gamma_\nu$, there exists a continuous function $\sigma : \mathbb{R}_{\geq 0} \to \mathbb{R}_{\geq 0}$ such that the time-reparametrized trajectory y', defined by $y'(t) := y(\sigma(t))$, satisfies $y' \in \Gamma_{\nu'}$. A direct consequence of this assumption is stated in the following lemma.

Lemma 3 *Suppose that the dynamics governing the bird has non-decreasing path sets with decreasing speed. Then, $\mathbb{P}\big(E_F(\nu)\big)$ is a non-increasing function of ν.*

Finally, the main result of this section, which follows directly from Lemmas 2 and 3, is stated below.

Theorem 4 *Suppose that the dynamics governing the bird, given by Equation* (1)*, is translation invariant and has non-decreasing path sets with decreasing speed. Then, there exists a critical speed ν_{crit}, possibly zero or infinity, such that*

- *for any speed $\nu > \nu_{\text{crit}}$, there exists no infinite trajectory for the bird that is collision free, almost surely,*
- *for any speed $\nu < \nu_{\text{crit}}$, there exists at least one infinite collision-free trajectory for the bird, almost surely.*

IV. Flight in a Poisson Forest

Theorem 4 established that, under mild technical assumptions, the existence of infinite collision-free trajectories exhibits a phase transition in any ergodic forest. However, the proof is not constructive in the sense that it does not compute the critical speed nor it provides any bounds. In this section, we employ percolation theory to provide lower and upper bounds on the critical speed for the special case of a single-integrator bird flying in a Poisson forest.

A. Percolation Theory

Before providing our main results, let us briefly interrupt the flow of the paper to introduce some important concepts in percolation theory. A couple of the definitions provided in this section will appear in the statement of our main results.

1) Discrete Percolation: An important model in percolation theory is the *site percolation on the square lattice*, described as follows. Let $\mathbb{Z}$ denote the set of integers and $\|\cdot\|_1$ denote the usual L_1 norm that gives rise to the Manhattan distance. Consider the graph that has vertex set $\mathbb{Z}^2$ and has an edge between $y_1, y_2 \in \mathbb{Z}^2$ whenever $\|y_1 - y_2\|_1 = 1$. This graph, called the *square lattice*, is illustrated in Figure 2. A sequence $(y_1, y_2, \ldots, y_k)$ of vertices is called a *path*, if y_i and y_{i+1} share an edge, for all $i \in \{1, 2, \ldots, k-1\}$.

Suppose each vertex in the square lattice is declared open with probability p and closed otherwise, independently from every other vertex. A path $(y_1, y_2, \ldots, y_k)$ is called an *open path*, if y_i is open for all $i \in \{1, 2, \ldots, k\}$. An *open cluster* is a maximal set of open vertices connected by open paths. An *infinite open cluster* is an open cluster with infinitely many vertices. Finally, the *site percolation* is said to occur, if the lattice contains an infinite open cluster.

Let V_p^0 denote the open cluster that contains the origin. We set $V_p^0 = \emptyset$ if the origin itself is closed. Note that the choice of origin is irrelevant here, since any vertex is statistically indistinguishable from any other. The *critical probability for site percolation* (on the square lattice) is defined as the smallest p such that the open cluster that contains the origin has infinitely many vertices, i.e., $p^s_{\text{crit}} = \inf\{p : \mathbb{P}(\{|W_p^0| = \infty\}) > 0\}$. It is rather easy to show that p^s_{crit} takes a non-trivial value, i.e., $p^s_{\text{crit}} \in (0, 1)$ [18]. What is more striking, however, is stated in the following theorem.

Theorem 5 ([18]) *In the site percolation model in the square lattice, there is no infinite open cluster, almost surely, for all $p < p^s_{\text{crit}}$; however, there exists a unique infinite open cluster, almost surely, for all $p > p^s_{\text{crit}}$.*

Although the precise value of p^s_{crit} is not known, rigorous bounds are available [18], and simulation studies suggest that p^s_{crit} is around 0.59274598 [22].

Percolation models on directed graphs are of particular interest for the purposes of this paper. A particularly important model is the directed hexagonal lattice shown in Figure 2. The site percolation model in the directed hexagonal lattice is similar to that on the (undirected) square lattice. Each vertex is declared open with probability p and closed otherwise. An open path is a directed path with every one of its vertices being open. The open cluster is defined similarly.

Theorem 5 is valid for site percolation on the directed hexagonal lattice also, albeit with a different percolation threshold, rigorous bounds for which are available [18]. In particular, it is known that the percolation threshold for this model is at most $\sqrt{3}/2$ [18].

2) Continuum Percolation: A continuum analogue of the site percolation model is the *Gilbert disk model*, described as follows. Recall that Π_λ denotes the (random) set of points generated by a Poisson process with intensity λ. Let $W_{\lambda,r}$ denote the region occupied by disks of radius r centered at the points generated by a Poisson process with intensity λ, i.e., $W_{\lambda,r} = \bigcup_{y \in \Pi_\lambda} B_r(y)$, where $B_r(y)$ denotes the Euclidean ball of radius r centered at y. The set $W_{\lambda,r}$ is also called the *occupied region*. An *occupied component* is a connected subset of $W_{\lambda,r}$ that is maximal with respect to set inclusion. Let $W^0_{\lambda,r}$ denote the occupied component that contains the origin. By convention, set $W^0_{\lambda,r} = \emptyset$ if the origin intersects no disk of the Gilbert disk model. An occupied component is said to be unbounded, if it has infinite Lebesgue measure, or equivalently if it can not be contained

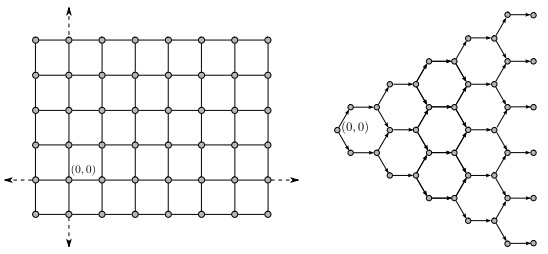

Fig. 2. The left and right figures illustrate a square lattice and a directed hexagonal lattice, respectively.

in any bounded subset of $\mathbb{R}^2$. Define the *critical intensity for occupied continuum percolation*, denoted by $\lambda_c(r)$, as the smallest intensity such that the occupied component that contains the origin is unbounded with non-zero probability, i.e., $\lambda_c(r) := \inf\{\lambda : \mathbb{P}(\{\mu(W^0_{\lambda,r}) = \infty\}) > 0\}$, where $\mu(\cdot)$ denotes the Lebesgue measure on $\mathbb{R}^2$.

As in the case of discrete percolation, it can be shown that $\lambda_c(r)$ takes a non-trivial value, i.e., $\lambda_c(r) \in (0, \infty)$ [19]. The theorem below is the continuum equivalent of Theorem 5.

Theorem 6 ([19]) *In the Gilbert disk model, there is no unbounded occupied component, almost surely, for all $\lambda < \lambda_c(r)$; however, there exists a unique unbounded occupied component, almost surely, for all $\lambda > \lambda_c(r)$.*

Continuum percolation phenomenon is known to depend on the intensity λ of the process and the radius r only through the expected number of points on a disk of radius r, i.e., $\lambda \pi r^2$. Strictly speaking, this quantity is the expected degree of a vertex in the graph formed by the Gilbert disk model, when two points with overlapping disks are joined by a vertex. That is, the *critical degree*, defined as $d_c := \lambda_c(r)\, \pi\, r$, is a constant function of r. Although the exact value of d_c is not known, rigorous bounds are available [18]. Using Monte-Carlo integration techniques, it was shown that d_c is between 4.508 and 4.515 with 99.99% confidence [23]. These results agree with the simulation studies which suggest that the critical degree lies between 4.51218 and 4.51228 [24].

Another model that is of particular interest for the purposes of this paper is one in which a square of side length l, instead of a disk, is placed on each point of the Poisson process. Due to the obvious analogy, this model will be called the *Gilbert square model*, which has also been studied extensively in the literature. In particular, Theorem 6 was shown to be valid for this model [18], and its critical degree was shown to be between 4.392 and 4.398 with 99.99% confidence [23].

B. On the Existence of Infinite Collision-free Trajectories

In this section, we provide lower and upper bounds on the critical speed for a single-integrator bird flying in a Poisson forest. Due to lack of space, we omit the proofs of the main results and refer the interested reader to [21].

Our first result is a lower bound on the critical speed. More generally, the following theorem provides a relation between the tree density ρ, the tree radius r, and the speed ν such that when this relation is satisfied there is at least one infinite collision-free trajectory through the forest, almost surely.

Theorem 7 *There exists an infinite collision-free trajectory of the single integrator bird, almost surely, whenever the tree density ρ, tree radius r, and the speed ν satisfy the following:*

$$\frac{\rho\, r^2}{\sin(\alpha)} < \log\left(1/\sqrt{p^{\mathrm{s}}_{\mathrm{crit}}}\right),$$

where $\alpha = 2\, \tan^{-1}(1/\nu)$ and $p^{\mathrm{s}}_{\mathrm{crit}}$ is the critical probability for site percolation on the directed hexagonal lattice.

In [21], we also show that in the regime considered in Theorem 7, the following holds. The probability that there exists an infinite collision-free trajectory that starts from a point within a distance of l to the origin is at least $1 - c_1 e^{-c_2\, l}$, where c_1 and c_2 are positive constants. In other words, in this regime, with very high probability, there exists an infinite collision-free trajectory for the bird starting from some point close to the origin.

The following theorem establishes a lower bound on the critical speed, again by providing a joint relation on ρ, r, and ν such that when the relation is satisfied there is no infinite collision-free trajectory for the single integrator bird through the Poisson forest, with probability one.

Theorem 8 *Suppose that the dynamics governing the bird is described by Equation* (2) *and the forest-generating process is Poisson with tree density ρ and tree radius r. Then, there exists no infinite collision-free trajectory, almost surely, whenever the ρ, r, and ν satisfy the following:*

$$\frac{\rho\, r^2}{\sin\alpha} > \frac{d_c}{2},$$

where $\alpha = 2\tan^{-1}(1/\nu)$ and d_c is the critical degree in the Gilbert square model.

In [21], we also prove the following claim. There exist positive constants c_3 and c_4 such that the probability that there exists a collision-free trajectory $y : [0, T] \to \mathbb{R}^2$ is at most $c_3\, e^{-c_4\, T}$. In other words, in this regime, it is very unlikely that the bird can fly for a long time without colliding with a tree.

V. Computational Experiments

This section is devoted to a Monte-Carlo simulation study that confirms the phase transition results established in the previous section. First, we provide a random geometric model in which a certain type of percolation occurs if and only if there exists an infinite trajectory for the single-integrator bird in a Poisson forest. Second, we use this percolation model in Monte-Carlo simulations to approximate the phase diagram of high-speed motion for the same special case.

A. An Equivalent Geometric Model

Consider a forest composed of a single tree with radius $r \in \mathbb{R}_{>0}$ located at $y \in \mathbb{R}^2$. Let $V_{\nu,r}(y)$ denote the set of all states starting from which the bird can not escape collision with this tree. The set $V_{\nu,r}(y)$ is illustrated in Figure 3. The set $V_{\nu,r}(y)$ is called the *left primary shadow region* of the tree with radius r located at y.

Consider a forest with two trees that are located at $y_1, y_2 \in \mathbb{R}^2$. Suppose both trees have radius r. Let $\mathcal{V}_{\nu,r}(\{y_1, y_2\})$ denote the set of all states starting from which collision is inevitable with either the tree located at y_1 or that located at y_2. In general, the set $\mathcal{V}_{\nu,r}(\{y_1, y_2\})$ is not the same as the set $V_{\nu,r}(y_1) \cup V_{\nu,r}(y_2)$.

Given a left primary shadow region $V_{\nu,r}(y)$, define the *top boundary* and the *bottom boundary* of $V_{\nu,r}(y)$ as shown

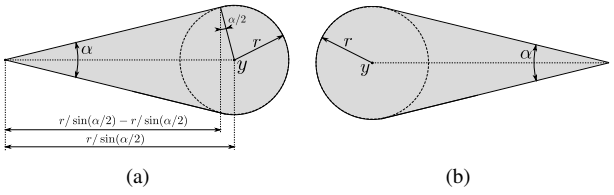

(a) (b)

Fig. 3. Figure (a) shows the left primary shadow region $V_{\nu,r}(y)$. The figure also illustrates the length of the region in terms of r and α. The right $W_{\nu,r}(y)$ primary shadow region is shown in Figure (b).

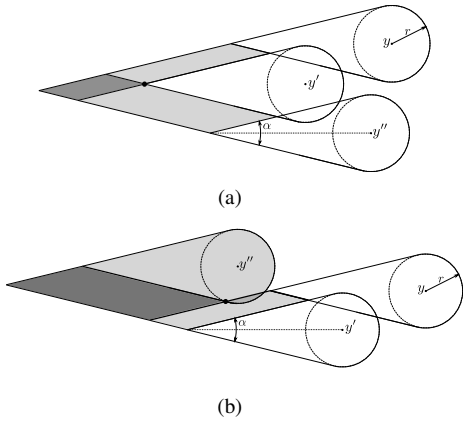

(a)

(b)

Fig. 5. In Figure (a), two induced shadows (shown in light grey) intersect to produce a new induced shadow region. Their point of intersection is shown by a black dot. In Figure (b), an intersection of an induced region and a primary shadow region is shown. The point of intersection is again shown as a black dot. The resulting induced shadow is in dark grey.

in Figure 4(a). Given two left primary shadow regions, say $V_{\nu,r}(y_1)$ and $V_{\nu,r}(y_2)$ as above, define the *left induced shadow region*, denoted by $\texttt{Ind}(V_{\nu,r}(y_1), V_{\nu,r}(y_2))$, as the set of all states starting from which the bird must go into either $V_{\nu,r}(y_1)$ or $V_{\nu,r}(y_2)$, thus eventually collide with either the tree located at y_1 or that located at y_2. See Figure 4(b). Notice that a left induced shadow region is formed only if the top boundary of one shadow intersects the bottom boundary of another shadow. If the opposite boundaries do not intersect, then the left induced shadow region is empty.

The top and bottom boundaries are defined for a left induced shadow region similarly as illustrated in Figure 4(c). In general, given two left shadows, say S_1 and S_2, either primary or induced, the set $\texttt{Ind}(S_1, S_2)$ is the set of all states starting from which the bird must either enter S_1 or S_2. The set $\texttt{Ind}(S_1, S_2)$ is nonempty whenever opposite boundaries of S_1 and S_2 intersect. See Figure 5 for an illustration.

Given a finite or a countably infinite set $\mathcal{Y} \subset \mathbb{R}^2$ of tree locations, let $\mathcal{V}_{\nu,r}(\mathcal{Y})$ denote the set of all states starting from which collision with some tree in $\mathcal{Y}$ is inevitable. In the sequel, $\mathcal{V}_{\nu,r}(\mathcal{Y})$ is called the *left shadow region* of the trees located at $\mathcal{Y}$ with radius r when the single-integrator bird is flying with longitudinal speed ν. If $\mathcal{Y}$ is a finite set, then $\mathcal{V}_{\nu,r}(\mathcal{Y})$ can be constructed in finite time by first constructing the induced left shadow regions of all pairs, then constructing the induced left shadow regions of all shadows, and so on, until there is no new induced shadow.

Given a tree of radius r located at y, let $W_{\nu,r}(y)$ denote the largest set of states that the bird can not reach starting from outside this set. The set $W_{\nu,r}(y)$, illustrated in Figure 3(b), is the mirror image of $V_{\nu,r}(y)$. Due to the obvious analogy, $W_{\nu,r}(y)$ is called the *right primary shadow region* of the tree with radius r located at r. The set $S_{\nu,r}(y) = V_{\nu,r}(y) \cup W_{\nu,r}(y)$ is called the *primary shadow region* of the same tree. The top boundaries of the primary shadow region is merely the union of the top boundaries of the left and right primary shadow regions. The bottom boundary is defined similarly. Given two shadow regions with intersecting opposite boundaries, their induced shadow regions can also be defined in the natural way. Given a finite set $\mathcal{Y}$ of tree locations and a tree radius, the set $\mathcal{S}_{\nu,r}(\mathcal{Y})$, called the *shadow region* corresponding to trees with radius r located at $\mathcal{Y}$, is computed by repeatedly constructing induced shadow regions until no more can be constructed.

The shadow region can also be constructed in a computably enumerable manner when $\mathcal{Y}$ is a countably infinite collection of points. Recall that Π_ρ denotes the (random) set of points generated by a Poisson process of intensity ρ. The region $\mathcal{S}_{\nu,r}(\Pi_\rho)$ is also called the *occupied shadow region*. The *vacant shadow region* is defined as $\mathbb{R}^2 \setminus \mathcal{S}_{\nu,r}(\Pi_\rho)$. An occupied shadow component is a subset of the shadow region that is maximal with respect to set inclusion. The reader is referred to [21] for an extensive study of this continuum percolation model, which we omit due to lack of space.

B. Results of Monte-Carlo Simulations

In the computational experiments, the existence of infinite collision-free trajectories is verified by testing the existence of trajectories crossing a large region. Let $\mathcal{R}(l, w)$ denote the region with width w (in the lateral direction) and length l (in the longitudinal direction) centered at the origin. Clearly, there exists a trajectory that crosses $\mathcal{R}(l, w)$ left to right if and only if the width of some occupied shadow component is equal to w.

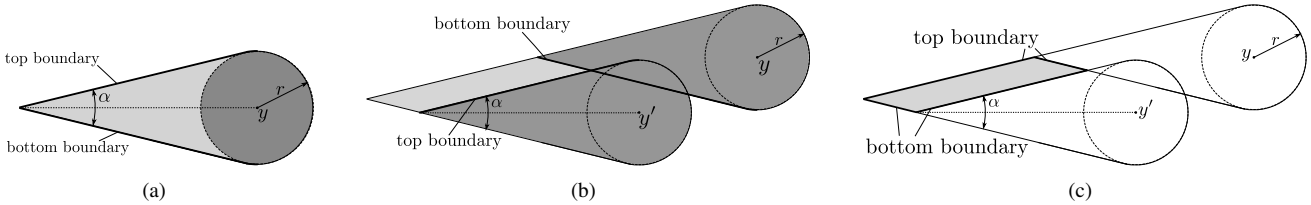

(a) (b) (c)

Fig. 4. In Figure (a), the top and the bottom boundaries of a primary left region are shown. In Figure (b) the induced shadow region is illustrated when the opposite boundaries two primary shadow regions intersect. In Figure (c), the top and bottom boundaries of the induced shadow region are illustrated.

In the experiments, the width of the test region is set to $w = 500$ and the length l is varied depending on the tree density ρ such that the expected number of trees in $\mathcal{R}(l, w)$ is equal to $50,000$, i.e., $\rho\, l\, w = 50,000$. In each experiment, the locations of the trees are generated according to a Poisson process restricted to $\mathcal{R}(l, w)$, the shadow region is computed, and the width of the largest-width occupied shadow component is noted after dividing it by w. This quantity will be called the *normalized maximum width*. To obtain a statistical distribution of the normalized maximum width, the experiment is repeated is repeated 200 times for each of several tree density and speed pairs. The set of all such pairs is shown in Figure 6. To give the reader an idea of what the shadow regions might look like, Figure 7 shows the shadow regions near the origin for three different velocities for the same realization of the Poisson forest.

In Figure 8, the distribution of the normalized maximum width, obtained from 200 independent trials for each tree density and speed pair, is illustrated for three select values of tree density, namely $\rho = 0.003, 0.01, 0.017$, and several values of speed. In Figure 9, normalized maximum width averaged over all trials is shown for each all of ρ-ν pairs that were considered in the experiments. The data is linearly interpolated for all other intermediate values.

It is clear from the figures that the maximum width changes rapidly near the critical speed. Thus, the experimental study confirms the phase transition right around the critical speed, which was predicted by the theory.

Finally, in Figure 10, the lower and upper bounds as predicted by Theorems 7 and 8 are given together with contour plots of the averaged normalized maximum width.

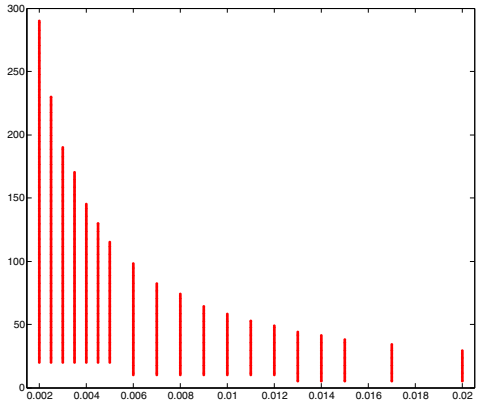

Fig. 6. The tree density (x-axis) and speed (y-axis) pairs that were considered in the computational experiment.

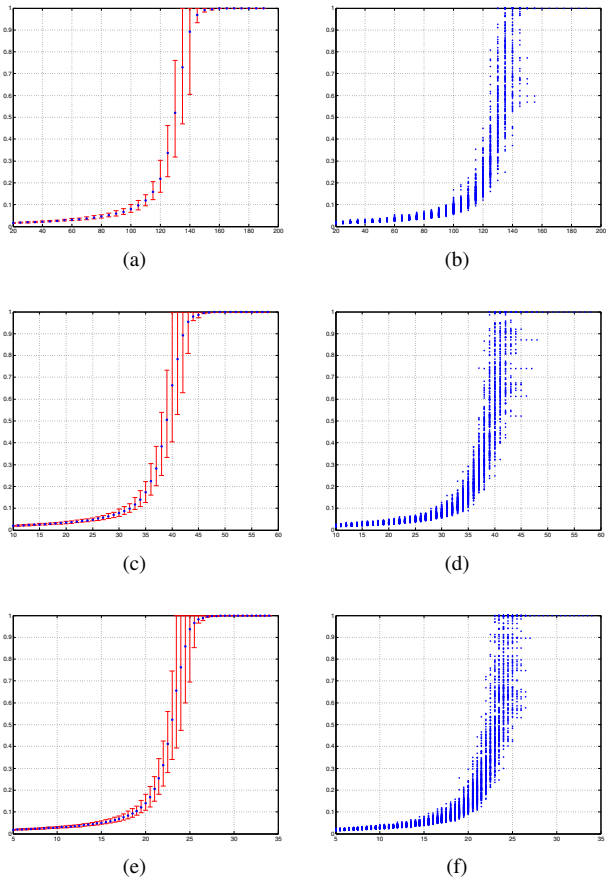

Fig. 8. Normalized maximum width versus the speed is shown for tree densities of 0.003, 0.010, and 0.017 in plots (a), (c), and (e), respectively. Average normalized maximum width values are shown in blue and the 10% and 90% percentiles of its distribution are shown by red bars. The distribution of the normalized maximum width are shown in scatter plots for the same tree densities in Figures (b), (d), and (f), respectively.

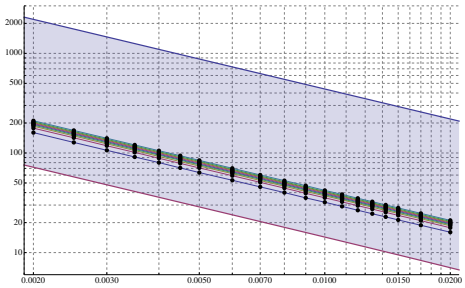

Fig. 10. Rigorous upper and lower bounds for the critical speed are shown together with the level sets of normalized maximum width obtained using computational experiments. Black dots represent the tree density and speed pairs corresponding to the averaged maximum width at several values ranging from 0.1 to 0.9 with increments of 0.1. The axes are in logarithmic scale showing tree density (x axis) versus the velocity (y axis).

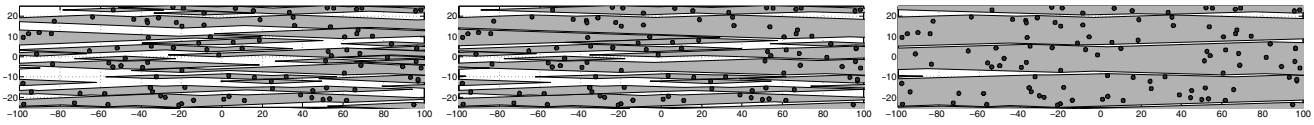

Fig. 7. A 200 meter by 50 meter portion of a particular realization of the Poisson forest with a tree density of 0.01 is shown. The trees are shaded in dark grey. The shadow regions are shown in light grey for velocities of 25, 30, and 35 in the left, center, and right figures, respectively. The white region is the set of all points starting from which flight with the corresponding speed can be maintained at least till the end of the 10,000-meters long region.

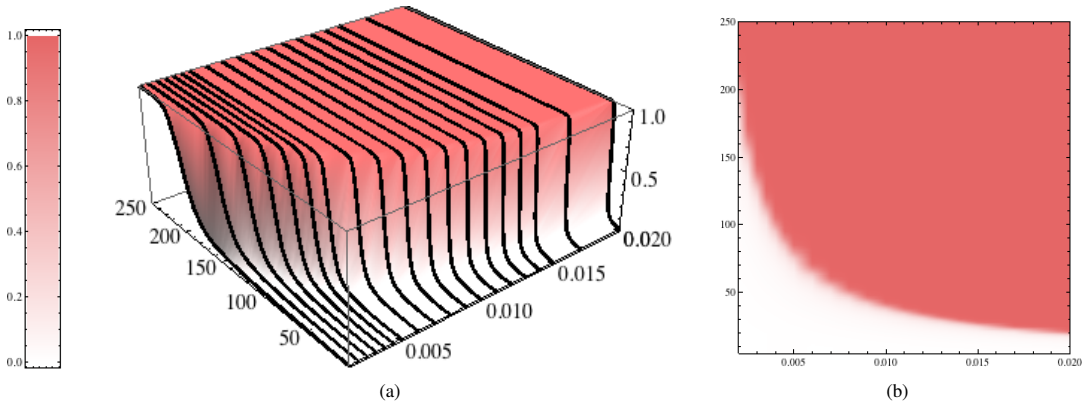

(a) (b)

Fig. 9. Normalized maximum width is shown for several values of the tree density and speed pairs in Figure (a). The black lines are linearly interpolated and extrapolated values obtained through computational experiments. The surface is a linear interpolation of the data represented by the black lines. The surface is color coded according to normalized maximum width. A legend for the color coding is given on the left. The top view of the surface presented in Figure (a) is shown in Figure (b), where the rapid transition from small values of the normalized maximum width to large values can be observed clearly.

VI. Conclusion

Largely inspired by birds flying at high speed through dense forests, this paper studied a novel infinite-horizon motion planning problem through randomly generated clutter. Our main result proves the existence of a phase transition, indicating fundamental limits of high-speed motion in randomly generated environments. More precisely, it is shown that, when the obstacle generation process is ergodic, there exists a critical speed such that motion with super-critical speed can not be maintained indefinitely, with probability one, although there exists at least one infinite collision-free trajectory in sub-critical speed conditions, almost surely. Lower and upper bounds for the critical speed were derived for an important special case using percolation theory. Moreover, results of extensive Monte-Carlo simulations are presented. The computational study confirms the aforementioned phase transition phenomenon.

There are many directions for future work. In particular, the authors believe that the case when the bird is endowed only with a limited sensing range is analytically tractable. The analysis presented in this paper may also be applied to several problems in a diverse set of fields ranging from mobile robotic networks to urban transportation. Future work will include exploring these potential application domains.

Acknowledgements

This work was partially supported by ONR MURI grant N00014-09-1-1051.

References

[1] D. Lentik and A. A. Biewener. Nature-inspired flight - beyond the leap. *Bioinspiration & Biomimetics*, 5(4), 2010.

[2] M. Selekwa, D. D. Dunlap, D. Shi, and E. G. Collins Jr. Robot navigation in very cluttered environments by preference-based fuzzy behaviors. *Robotics and Autonomous Systems*, 56(3):231–246, 2008.

[3] K. Yang and S. Sukkarieh. 3D Smooth Path Planning for a UAV in Cluttered Natural Environments. In *2008 IEEE/RSJ International Conference on Intelligent Robots and Systems*, 2008.

[4] D. Shim, H. Chung, and S. S. Sastry. Conflict-free Navigation in Unknown Urban Environments. *IEEE Robotics and Automation Magazine*, 2006.

[5] J. Langelaan and S. Rock. Towards Autonomous UAV Flight in Forests. In *AIAA Guidance, Navigation and Control Conference*, 2005.

[6] D. Shim, H. Chung, H. J. Kim, and S. Sastry. Autonomous Exploration in Unknown Urban Environments for Unmanned Aerial Vehicles. In *AIAA Guidence Navigation and Control Conference*, 2005.

[7] BBC Worldwide Documentary. Flying with the fastest birds on the planet: Peregrine Falcon & Gos Hawk.

[8] A. Hedenstrom and T. Alerstam. Optimal Flight Speed of Birds. *Philosophical Transactions of the Royal Society B: Biological Sciences*, 348:471–487, 1995.

[9] C. P. Ellington. Limitations on Animal Performance. *Journal of Experimental Biology*, 160(71-91):1–22, 1991.

[10] B. W. Tobalske, T. L. Hedrick, K. P. Dial, and A. A. Biewener. Comparative power curves in bird flight. *Nature*, 421(6921):363–366, January 2003.

[11] A. A. Biewener, W. R. Corning, and B. W. Tobalske. In Vivo Pectoralis Muscle Force-length Behavior During Level Flight in Pigeons (Columba Livia). *The Journal of Experimental Biology*, 201:3293–3307, 1998.

[12] T. L. Hedrick and A. A. Biewener. Low speed maneuvering flight of the rose-breasted cockatoo (Eolophus roseicapillus). I. Kinematic and neuromuscular control of turning. *Journal of Experimental Biology*, 210(11):1897–1911, June 2007.

[13] T. L. Hedrick, J R Usherwood, and A. A. Biewener. Low speed maneuvering flight of the rose-breasted cockatoo (Eolophus roseicapillus). II. Inertial and aerodynamic reorientation. *Journal of Experimental Biology*, 210(11):1912–1924, June 2007.

[14] B. Husch, T. W. Beers, and J. A. Kershaw. *Forest mensuration*. Wiley, 2003.

[15] D. Stoyan and A. Penttinen. Recent Applications of Point Process Methods in Forestry Statistics. *Statistical Science*, 15(1):61–78, 2000.

[16] E. Tomppo. *Models and methods for analysing spatial patterns of trees*. PhD thesis, Communicationes Instituti forestalis Fenniae, 1986.

[17] P. Walters. *An introduction to ergodic theory*. Springer Verlag, October 2000.

[18] B. Bollobás and O. Riordan. *Percolation*. Cambridge Univ Pr, 2006.

[19] R. Meester and R. Roy. *Continuum percolation*. Cambridge Univ Pr, 1996.

[20] D. J. Daley and D. Vere-Jones. *An Introduction to the Theory of Point Processes: General theory and structure*. Springer Verlag, November 2007.

[21] S. Karaman and E. Frazzoli. High-speed Flight in an Ergodic Forest. arXiv:1202.0253, http://arxiv.org/abs/1202.0253, 2012.

[22] M. J. Lee. Pseudo-random-number generators and the square site percolation threshold. *Physical Review E*, 78, 2008.

[23] P. Balister, B. Bollobás, and M. Walters. Continuum percolation with steps in the square or the disc. *Random Structures & Algorithms*, 26(4):392–403, 2005.

[24] J. Quintanilla and S. Torquato. Efficient measurement of the percolation threshold for fully penetrable discs. *Journal of Physics A: Mathematical and General*, 33:399–407, 2000.